Sustainability, Agri, Food and Environmental Research, (ISSN: 0719-3726), 11(X), 2023:
http://dx.doi.org/10.7770/safer-V11N1-art2722

Ultrafiltration of Moroccan Valencia orange juice: juice quality, optimization by custom designs and membrane fouling

Ultrafiltración del zumo de naranja Valencia marroquí : calidad del zumo, optimización mediante diseños personalizados y ensuciamiento de las membranas

F.Z. Addar[1], S. Qaid[3], H. Zeggar[1], H. El Hajji[2], M. Tahaikt[1], A. Elmidaoui[1], M. Taky*[1,4]

[1]Laboratory of Advanced Materials and Process Engineering, Faculty of Sciences, Ibn Tofail University, BP 1246, Kenitra - Morocco

[2]Electrochemistry and Analytical Chemistry Team, Mohammed V University, Rabat - Morocco

[3]Department of industrial chemistry, Faculty of Applied Sciences, Taiz University - Yemen.

[4] International Water Research Institute, Mohammed VI Polytechnic University, Lot 660, Hay Moulay Rachid Ben Guerir, 43150 - Morocco

Emails address: mohamed.taky@uit.ac.ma, takymohamed@gmail.com, *Corresponding author

Abstract

The growing demand for healthy foods has forced researchers to develop processes capable of concentrating or clarifying fruit juices while producing high quality products and the most promising techniques are membrane techniques. However, the obstacle of these techniques is the fouling problem. The objective of this study is to clarify Moroccan Valencia orange juice by ultrafiltration (UF) using two plate membranes characterized by different membrane materials (polyether sulfone (PES) and polysulfone (PS) with a molecular weight cutoff (MWCO) of 30 and 20 k Da respectively. The performance of these membranes was studied in terms of selectivity and productivity in respect to parameters describing juice quality. In the first part of this work, the response surface method (RSM) based on custom designs (CD) was used to model and optimize the UF process. The independent variables of the RSM method are transmembrane pressure (TMP) and feed flow rate (FF), while permeate flux is considered as a response. Secondly, Hermia model and resistance model were applied to describe and to identify the fouling mechanism. According to the results, the two membranes kept the original composition while the total suspended solids (SS) and the pectin content were completely removed. Both factors (TMP) and (FF) influence significantly the permeate flux. A TMP of 1.99-2 bar and FF of 229.99-330 L/h for PES and PS respectively were obtained. ANOVA of the regression model showed that both models are highly significant with $R^2 > 0.95$. However, the PES membrane exhibits a permeate flux which is greater than the PS membrane. The rejection rates of the monitored parameters were lower than those obtained by the PS membrane. The concentration polarization is the main cause of the flux drop and it appears that, for both membranes, the fouling is due to surface fouling mechanisms which is a cake formation.

Keywords: Ultrafiltration, Valencia orange juice, Quality, Response surface methodology, Custom designs, Membrane transfer, Membrane fouling, Modelisation.

Resumen

La creciente demanda de alimentos saludables ha obligado a los investigadores a desarrollar procesos capaces de concentrar o la clarificación de los zumos de fruta produciendo productos de alta calidad y las técnicas más prometedoras son las de membrana. Sin embargo, el obstáculo de estas técnicas es el problema del ensuciamiento. El objetivo de este estudio es clarificar el zumo de naranja Valencia marroquí mediante ultrafiltración (UF) utilizando utilizando dos membranas de placa caracterizadas por diferentes materiales de membrana (poliéter sulfona (PES) y polisulfona (PS) con un corte de peso molecular (MWCO) de 30 y 20 k Da respectivamente. El rendimiento de estas membranas se estudió en términos de selectividad y productividad con respecto a los parámetros que describen la calidad del zumo. En la primera parte de este trabajo, se utilizó el método de superficie de respuesta (RSM) basado en diseños personalizados (CD) para modelar y optimizar el proceso de UF. Las variables independientes del método RSM son la presión transmembrana (TMP) y el caudal de alimentación (FF), mientras que el flujo de permeado se considera una respuesta. En segundo lugar, se aplicó el modelo Hermia y el modelo de resistencia para describir e identificar el mecanismo de ensuciamiento. Según los resultados, las dos membranas mantuvieron la composición original, mientras que el total de sólidos en suspensión (SS) y el contenido de pectina se eliminaron por completo. Ambos factores (TMP) y (FF) influyen significativamente en el flujo de permeado. Se obtuvo una TMP de 1.99-2 bar y un FF de 229.99-330 L/h para PES y PS respectivamente. El ANOVA del modelo de regresión mostró que ambos modelos son altamente significativos con $R^2 > 0.95$. Sin embargo, la membrana PES presenta un flujo de permeado mayor que la membrana PS. Los índices de rechazo de los parámetros controlados fueron inferiores a los obtenidos por la membrana de PS. La polarización de la concentración es la principal causa de la caída del flujo y parece que, En el caso de ambas membranas, el ensuciamiento se debe a mecanismos de ensuciamiento superficial, es decir, a la formación de una torta.

Palabras clave: Ultrafiltración, Zumo de naranja de Valencia, Calidad, Metodología de superficie de respuesta, Diseños personalizados, Transferencia de membranas, Ensuciamiento de la membrana, Modelización.

Introduction

Nowadays, there is a growing global trend to consume tropical fruits, juices and fruit drinks as they are seen as a healthier option for health. The process of producing fruit juice is generally comprised of several stages such as washing, crushing, husking, pressing, clarifying, pasteurizing, and storing. Fruit juices are typically concentrated by multi-stage vacuum evaporation to reduce storage and shipping costs. However, industrial heat treatments can have negative impacts on nutrient components as well as result in loss of fresh juice aromas, color degradation and a cooked taste (Jiao et al., 2004; Mangindaan et al., 2018). Traditional methods of clarification

have been concentrated by multi-stage vacuum evaporation, such as enzymatic treatment (depectinization), cooling, flocculation (gelatin, silica sol, bentonite and diatomaceous), decantation and filtration (Conidi et al.,2020). These processes use large amounts of additives which causes environmental problems and significant disposal cost with other disadvantages, such as the risk of dust inhalation caused by handling and disposal, environmental issues (Noble, and Stern, 2020). The growing demand for healthy foods has forced researchers to develop alternative processes capable of concentrating or clarifying fruit juice while producing high quality products. The most promising alternative is membrane-based techniques (Toledo Guimarães et al., 2018).

Membrane processes such as reverse osmosis (RO), ultrafiltration (UF), microfiltration (MF) and nanofiltration (NF) appears as an alternative to traditional techniques for clarifying and concentrating fruit juices. In addition to being economical and environmentally friendly, these separation techniques allow the production of high-quality products thanks to their high selectivity and low operating temperatures. They retain the flavor, aroma, appearance and mouthfeel of freshly squeezed juices in the concentrate and ultimately in the reconstituted juice (Medina and Garcia, 1988; Arriola et al., 2014). In particular, UF avoids the use of traditional fining agents which pose environmental impact problems due to their elimination; the separation is athermal allowing efficient separation and concentration of solutes without changing phase and preserving the chemical, physical and nutritional properties of food components without harmful chemical addition (Cassano et al., 2007). The application of UF for fruit juices has been largely studied for the juices of apple, orange, guava and kiwifruit with the focus on different processing parameters (feed concentration, operating pressure, feed pH, cross-flow velocity, temperature etc…) and juice quality attributes (clarity, color, pH, nutritional content etc…) (Cassano et al.,2007; Medina and Garcia,1988).

Despite the progress made in UF processes, fouling is the most serious problem that negatively affects the membrane performances in the fruit juice industry, for instance: reduction in the active area of the membrane, decline of flux, increase in operating pressure, energy consumption and treatment cost. This phenomenon is influenced by many factors such as nature and concentration of solutes and solvents, membrane type, pore size distribution, surface characteristics, membranes materials, and hydrodynamics of membrane module (Cassano et al.,2007; Cassano et al.,2011).

Usually, fouling occurs following deposition of foulants species on the membrane surface (cake formation) or by physicochemical interactions with the membrane such as adsorption on the porous walls of the membrane and the closing of the pores (pore blocking) (Cassano et al.,2006). Each foulants results in a particular fouling mode: macromolecules lead to gel or cake formation on membrane, macromolecular fouling within the structure of porous membranes (Carneiro et al.,2002), small colloidal particles can rise to a fouling layer, small organic molecules tend to have strong interactions with polymer membranes; large suspended particles which are present in the original feed or developed in the process by scaling can block module channels (Qaid et al.,2017), proteins lead to interactions with surface or pores of membranes (Qaid et al.,2017), chemical reactions can lead to

precipitation of salts and hydroxides due to concentration and pH increase (Qaid et al.,2017), biological reactions lead to the growth of bacteria on the membrane surface and excretion of extracellular polymers substances (Gulec et al.,2018). Cake formation and pore-blocking result in flux decline with the processing time, thus reducing the permeability of the membrane or making a thin layer over the membrane surface introducing an additive resistance to transfer. Membrane fouling controls the frequency of cleaning, the lifetime of the membrane, area needed for separation which ultimately determines the costs, design and operating parameters of membrane plants (Omar et al.,2020).

The construction of mathematical models for the prediction of membrane separation processes is a valuable tool in the field of membrane science and technology. Its play an important role in the simulation and optimization of membrane systems, leading to efficient and economical designs of separation processes (Montgomery, 2011; Myers and Montgomery, 2001; Addar et al., 2021). Response surface methodology (RSM) is an efficient statistical analysis method that improves and solves all the drawbacks identified in the classical methods (Addar et al., 2021). RSM is typically used to locate the optimal process parameters to achieve the target mean value assuming homogeneous variances (Khuri and Cornell,1996; Box and Draper,2007). RSM derives the model between the response and a number of input variables. Typically, a second-order model is used to derive the order model is used to derive the empirical relationship, based on the ordinary least squares method, assuming that the observations are independent and the variances are homogeneous. Some types of RSM used in the literature to model the physical-chemical process include the Central Composite Design (CCD), Boxe-Behnken Design (BBD), User-Defined Design, and Customized Historical Data Model (Hussain et al.,2021).

To deal with the problem of fouling researchers thought to control the fouling by mitigation techniques by adding anti-foulant or hydrophobic chemicals to the feed for stopping fouling-inducing mechanisms, by regular cleaning and optimizing the duration of the operation cycle. Modeling fouling and prediction algorithms also gives the possibility to control it well and reduce its effects: These algorithms have predominantly been based on empirical approaches or mathematic models.

The aim of this study is to clarify a Moroccan Valencia orange juice by UF using two flat sheet membranes (polyethersulfone (PES) and polysulfone (PS) with molecular weight cut-off (MWCO) 30 and 20 kDa respectively. The performance of selected membranes is investigated in terms of selectivity and productivity towards color, pectin content (AIS) and suspended solids (SS). RSM based on custom designs, is adopted to optimize the transmembrane pressure (TMP) and (FF) by maximizing the permeate flux for both membranes. The effect of variables on the response is evaluated in terms of response graphs. In addition, to identify the type of fouling, the permeate flux is tracked as a function of time and then modeled using the Hermia model. To quantify the resistance of the different fouling (internal and external), an experimental method is adopted which consists in determining the total resistance of the membrane (Rt) after the UF separation from the value of the permeate flux measured on the basis of Darcy's law.

Materials and methods

A. Experimental method: Valencia orange juice is prepared and depectinized in the laboratory from fresh fruit grown at the Regional Center for Agricultural Research in Kenitra (Morocco). Fruits are manually washed with water in order to remove surface dirt. Then, they are cut crosswise and squeezed by a domestic juicer. The squeezed juice is depectinized by using a commercial pectinase from *Aspergillus aculeatus* (Pectinex® Ultra SPL from Aspergillus Aculeatus, Sigma-Aldrich), which is added in a quantity of 20 mg/L. The enzyme is able to hydrolyze both high and low esterified pectins and also partially hydrolyze cellulose and hemicellulose (Qaid et al.,2017). The juice is incubated for 4 h at room temperature in plastic tanks and then filtered with a nylon cloth. The depectinized juice is stored at -20 °C and is defrosted to room temperature before the UF treatment.The method is already described in an previous article by Qaid et al.(2017). The Table 1 gives the physico-chemical characteristics of Valencia orange juice depectinized.

UF tests are carried out on depectinized juice at 27°C. The parameters followed are: color, clarity, total soluble solids (TSS), suspended solids content (SS), pH, acidity, viscosity, density and pectin content (AIS), is shown in Table 1.

Table 1: Characterization of valencia orange juice depectinized.

Characteristic	Valencia orange juice depectinized
pH	3.32
Density (g/cm^3)	1.08
Viscosity (mPa.s^{-1})	1.45
Color (A420)	0.76
Clarity (%T_{660})	45.57
Acidity (% CA)	1.02
TSS (°Brix)	11.09
SS (w/w%)	4.12
AIS (wt%)	0.19

The pilot used is a cross-flow filtration laboratory pilot supplied by Sterlitech Corporation (Sterlitech Corporation, WA, USA), equipped with a Sepa CF membrane cell system figure 1.

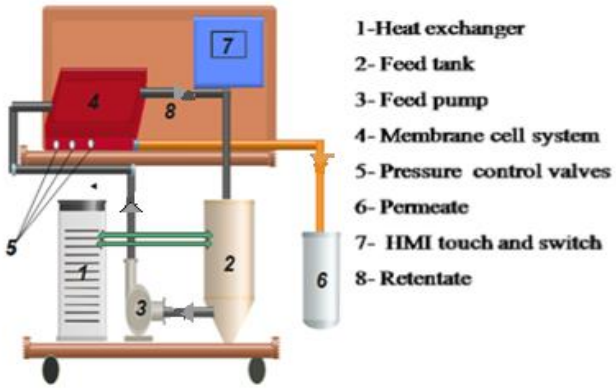

Figure 1: Scheme of the UF pilot laboratory

The juice is analyzed for color, clarity, TSS, SS, pH, acidity, viscosity, density, pectin content (AIS). Color and clarity of the juice are evaluated by measuring the absorbance at 420 nm and transmittance at 660 nm, respectively, using a UV/Vis spectrophotometer (SPECORD® 210 PLUS, analyticjena, Germany). TSS content is measured, using a ATAGO digital refractometer (Atago Co., Ltd., Tokyo, Japan) and the results are expressed as °Brix. The pH of the solutions is measured using a pH meter (Hanna Instruments., HI2221, USA) at 25°C. Viscosity is measured by using a FUNGILAB viscometer (Barcelona, Spain). The density of juice is determined using 25 mL juice by volumetric flask of 25 mL and precision balance. The SS is determined with the total juice relation (%w/w) by centrifuging, at 2000 rpm for 20 min, 45 mL of a pre-weighted sample; the weight of settled solids is determined after removing the supernatant. The content of pectic materials is measured in terms of AIS. AIS values are determined by boiling 20 g juice with 300 mL of 80% alcohol solution and simmering for 30 min (Qaid et al.,2017).

UF's operations are conducted according to two configurations: Batch system and semi-batch system. The membranes tested are flat membranes with dimensions of 190 × 140 mm and an effective surface area of 0.014 m^2. They are supplied by Sterlitech Corporation (WA, USA). Their characteristics are reported in Table 2.

Table 2: Charateristics of flat sheet UF membranes.

Manufacturer	Designation	Material	MWCO (kDa)	Operating Ph
Nanostone	PS35	PS	20	1-10
Synder	MK	PES	30	1-11

Volume reduction factor (VRF) is defined as the ratio between the initial feed volume and the final retentate volume, according to the following equation:

$$VRF = \frac{V_f}{V_r} = 1 + \frac{V_p}{V_r} \qquad (eq.1)$$

Where V_f, V_r, and V_p are the volume of feed, retentate, and permeate, respectively.

The recovery rate (Y) is calculated as follow:

$$Y = \frac{Q_p}{Q_f} * 100 \qquad (eq.2)$$

Where Q_p is permeate flow, Q_f is initial feed flow.

The retention R of UF membranes towards specific compounds is calculated as follow:

$$R = 100 * \left(1 - \frac{C_p}{C_f}\right) \qquad (eq.3)$$

Where C_p and C_f are the concentrations of specific component in the permeate and feed, respectively.

The hydraulic permeability of each membrane is determined by the slope of the straight lines obtained by plotting the water flux values in selected operating conditions versus the applied TMP ΔP. The permeation process across the membrane can generally be described by Darcy's law as follow:

$$J = \frac{Q}{S} = \frac{\Delta P}{\mu . Rm} = L_P * \Delta P \qquad (eq.4)$$

Where J ($m.s^{-1}$) is the permeation flux, Q ($m^3.s^{-1}$) is permeate flow, S (m^2) is surface of the membrane, ΔP (bar) is the TMP, μ (Pa.s) is the viscosity of the permeate and R_m (m^{-1}) is the resistance to the permeate and L_p ($m.s^{-1}.bar^{-1}$) is the membrane permeability.

B.RSM statistical analysis method: The RSM aims to optimize the response surface controlled by the process parameters, and it is a flexible optimization method. The factors can be both numerical and categorical and the type of numerical factors can be changed from continuous to discrete and can estimate linear, interaction and quadratic effects of parameters (Liu et al.,2018). A custom historical design approach applied in the present work is a subset of RSM and is used to configure the relationship between the operational variables and the responses. To this end, previously performed experimental data (16 experimental cycles) containing two input variables (TMP (X1) and FF (X2)) and one response permeate flux (PF) as presented in Table 3, are imported into the Design Expert software (version 13) to describe the governed performance in the UF process for both membranes (PES and PS). A quadratic polynomial model was used in this study, as presented in equation (5).

$$Y = a_0 + a_1X_1 + a_2X_2 + a_3X_1X_2 + a_4X_1^2 + a_5X_2^2 \qquad \text{(eq. 5)}$$

Where Y is the output variable, a_0 , a_1 , a_2 , a_3 , a_4 , a_5 are the regression coefficients. Coefficients with one factor represent the effect of the particular factor, while coefficients with two factors and those with second order terms represent the effect of the factor.

The coefficient of determination R^2 indicates the quality of the polynomial. The performance of the model is verified by analyzing its results by ANOVA. Recently research studies have suggested that, model significance and non-significant lack of fit are the two main approaches qualified for any response prediction to represent the degree of fit between the predicted model and the experimental work (Maghsoudy et al.,2019; Chen et al.,2018).

Table 3: Design Experimental Data.

Experiment Number	Input variables PES and PS membrane		Output variable	
	X1 (bar)	X2 (L/h)	PF ($L/m^2.h$) PES	PF ($L/m^2.h$) PS
1	0.5	134	17.5	10
2	0.5	150	21	12.98
3	0.5	190	23.61	16.38
4	0.5	230	30.15	23.61
5	1	134	26	17
6	1	150	28.23	20.34
7	1	190	35.86	27.43
8	1	230	40.91	31.77
9	1.5	134	31	24.16
10	1.5	150	34.49	26.73
11	1.5	190	44.85	31.65
12	1.5	230	49.22	38.18
13	2	134	34.5	29
14	2	150	44.5	32.3
15	2	190	51.25	38.21
16	2	230	58.75	44.16

RESULTS AND DISCUSSION

A. Effect of TMP and FF

In order to determine the optimal pressure and FF, the statistical method of optimization based on the RSM and UF experiments are performed in the batch configuration mode for the two UF membranes tested. The parameter monitored is the permeate flow rate.

Figures 3 and 6 show the response surface plot for the interaction effects of the FF and TMP parameters on permeate flow for the two membranes tested. Table 4 shows the ANOVA results for the response of the PES and PS membranes.

The statistical estimators calculated by the mathematical methodology are sum of squares (SS_S), mean squares (MS), degree of freedom (DF), F-value, p-value and R-squared, etc. From a statistical point of view, the F-values for the two models (PES, PS) of 155.34-382.39 respectively and the p-values less than 0.0001 obtained imply that both models are significant and that there is only 0.01% chance that an error could occur due to noise. In

general, p-values less than 0.0500 indicate that the model terms are significant, otherwise the model is insignificant Addar et al., (2021). On the other hand, the R^2 values obtained, as well as the predicted and adjusted R^2 coefficient for both models are higher than 0.95. This shows a good agreement between the results obtained experimentally and by modeling. These two regression models can be applied as adequate and valid models to predict and simulate the UF process as a function of the independent variables.

The regression equations for the generated permeate flux for PES and PS are equations (6)-(7) presented as follows:

$$Y_{PES} = 38.61 + 12.28X_1 + 8.52X_2 + 2.62X_1X_2 - 1.31X_1^2 - 1.7X_2^2 \quad \text{(Eq. 6)}$$

$$Y_{PS} = 28.30 + 10.03X_1 + 7.05X_2 + 0.3675X_1X_2 - 1.49X_1^2 - 0.1496X_2^2 \quad \text{(Eq. 7)}$$

Table 4: ANOVA for the quadratic model.

Model	Sum of Squares	dF	Mean Square	F-value	p-value		R^2	R^2-predicted	R^2- Adjusted
PES	2017.42	5	403.48	155.34	< 0.0001	significant	0.9628	0.9809	0.9628
PS	1372.82	5	274.56	382.39	< 0.0001	significant	0.9948	0.9922	0.9879

Figures (2a,5a) show the plots of the residuals as a function of the order of observation for both membranes, these residuals are the difference between the predicted and real values and should follow a normal distribution if the experimental errors are random. The fit of the model in terms of the residuals should follow a straight line (Dessie et al.,2020), which in our situation leads to the conclusion that the errors are normally distributed. That is, all residuals are not correlated with each other as an effect during positive and negative distributions of residuals. Therefore, the distribution of an experimental series across these lines follows a normal distribution at the limit of the 95% confidence interval. Thus, a randomization of experimental data points along the horizontal line of residuals suggests that the proposed models are adequate, and this claim is also supported by other studies (Dessie et al.,2020, and Mondal and Purkait, 2017).

For Figures (2b,5b) the real values are distributed relatively close to the line of predicted values, showing that there is a good correlation between the real and predicted values for both membranes.

From Figures 3 and 6, TMP and FF rate influence the permeate flow rate. The behavior of the two membranes is similar. For both membranes the TMP contributes significantly to the permeate flux. When the TMP is increased from 0.5 to 2 bar, the permeate flux increased. following Darcy's law (Lin et al.,2020). The permeation flux of the PES membrane is greater than that of the PS membrane. The phenomenon that controls the flow rate of permeate through the two membranes tested in the applied TMP range is concentration polarization which occurs when the feed solution containing suspended and soluble solids (colloids). According to the concentration

polarization model of the gel, the formation of a viscous and gelatinous layer is responsible for additional resistance to permeate flow in addition to that of the membrane (Drioli et al.,2017). However, for the two membranes studied, an increase in the feed flow rate leads to higher permeate flux. According to the film model, an increase in the recirculation velocity improves hydrodynamic conditions, reduces polarization thickness layer and concentration polarization, so the mass transfer coefficient is enhanced and the permeation flux increases (Qaid et al.,2017; Nilsson, 1990).

RSM is used to fit a quadratic model to optimize the dependent parameters based on the values of the independent variables obtained from the experimental data (Najafi et al.,2018). Figures 4 and 7 show the results of RSM optimization for both membranes by maximizing the permeate flux under the optimal conditions for each independent variable. Each graph includes the predictions X1 and X2, whose values are optimized with respect to the permeate flux value, where X1 refers to the horizontal axis (TMP) and X2 to the vertical axis (FF). The optimal values obtained X1 is 1.99 and 2 and for X2 is 229.99 and 230 for PES and PS respectively. These results are confirmed by the desirability values. If the value is close to zero, the response is totally unaccepted, and if the value is close or equal to 1, the response is accepted (Boumaaza et al.,2020). These results are selected for the best set of physico-chemical variables that correspond to the best desirability, as shown in Figures 4 and 7.

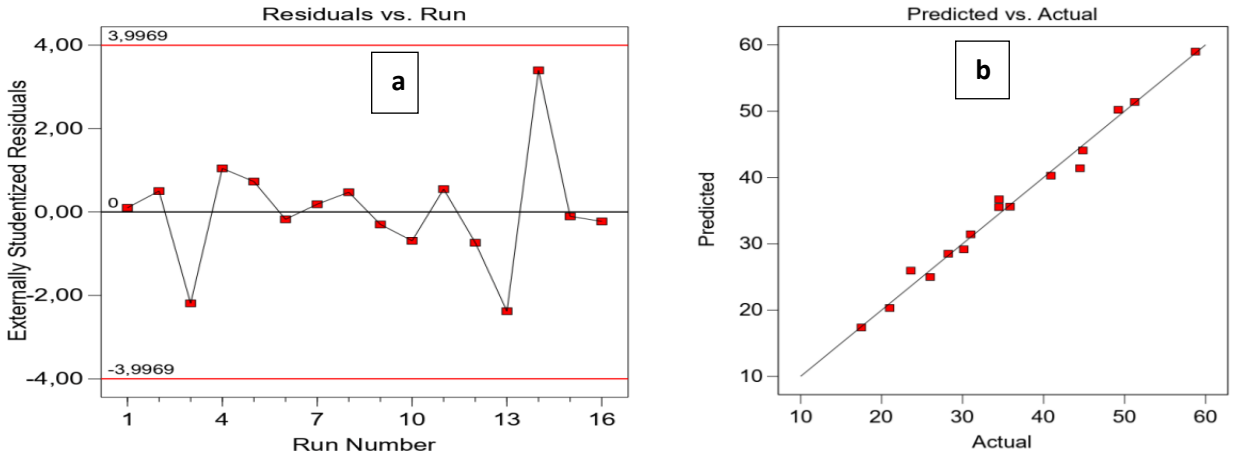

Figure 2: Plot of residuals versus observation order (a) and Relationship between predicted and experimental values of permeate flux (b) for the PES membrane.

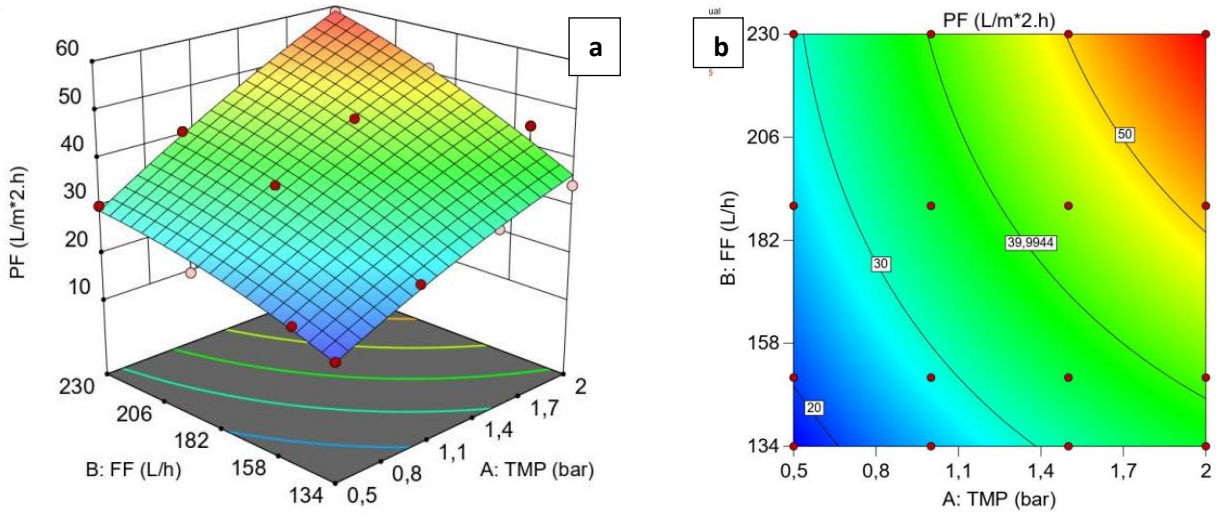

Figure 3: 3D response surface (a) and 2D contour plot for the interaction effect of two parameters on the response (b) for the PES membrane.

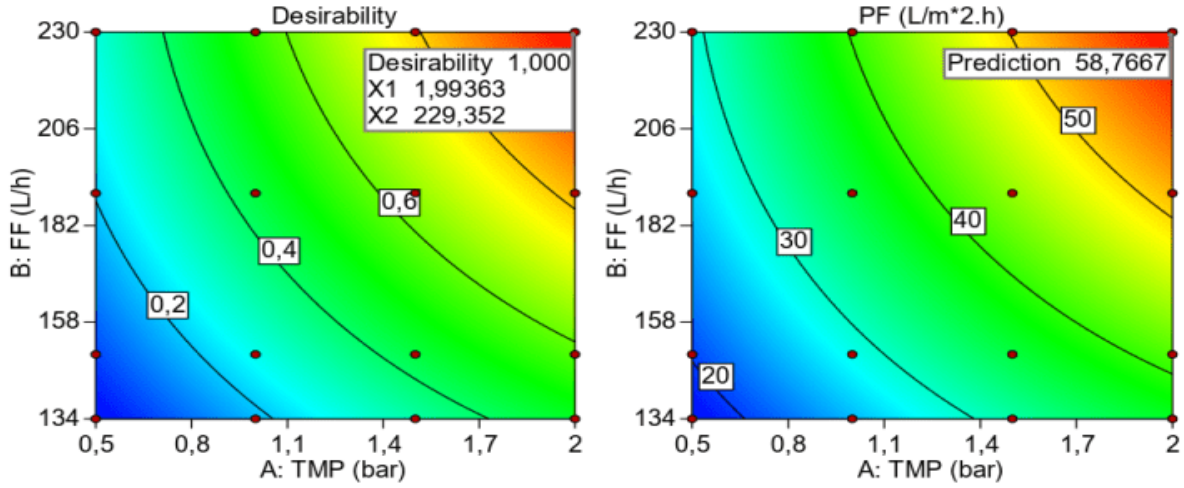

Figure 4: Optimum conditions for the permeate flux maximization for PES membrane.

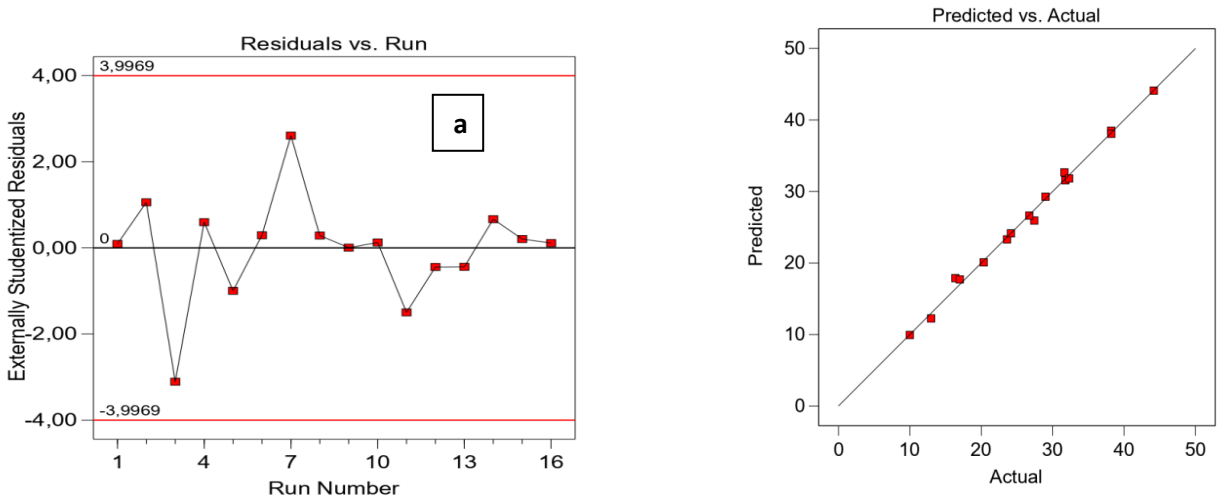

Figure 5: Plot of residuals versus observation order (a) and Relationship between predicted and experimental values of permeate flux (b) for the PS membrane.

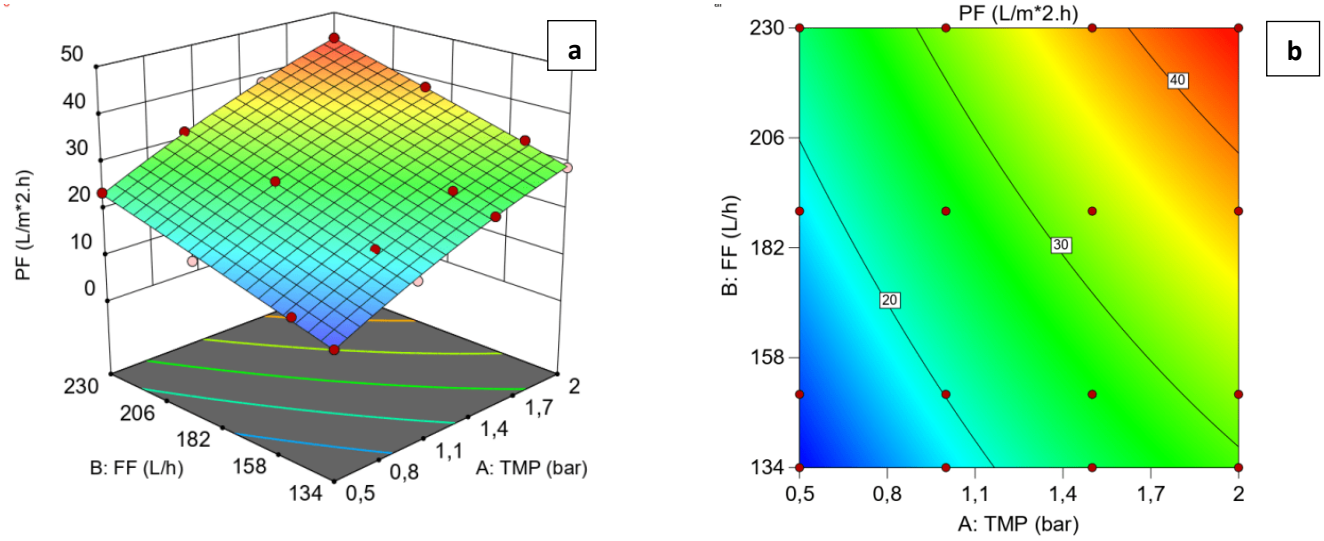

Figure 6: 3D response surface (a) and 2D contour plot for the interaction effect of two parameters on the response (b) for the PS membrane.

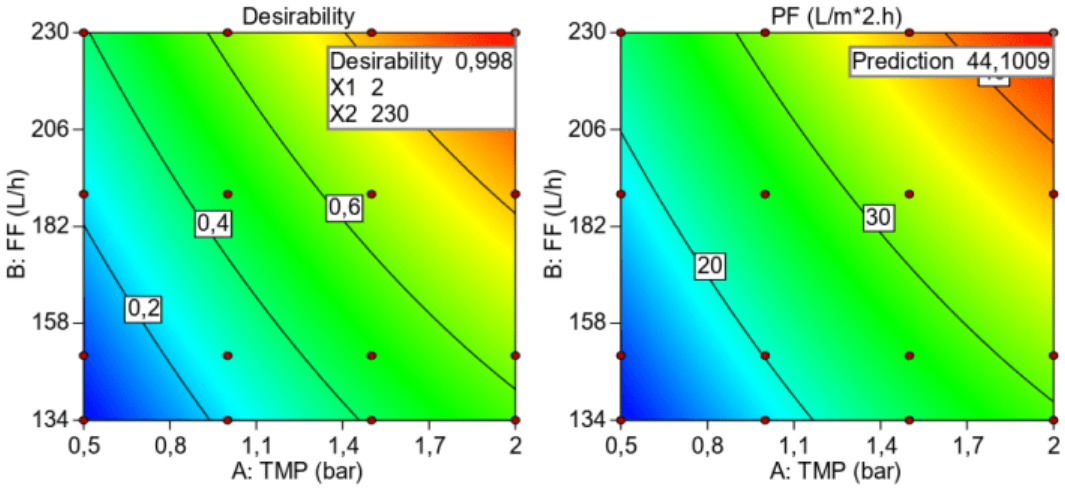

Figure 7: Optimum conditions for the permeate flux maximization for PS membrane

B. Effect of VRF and fouling identification

B.1 Effect of VRF

The influence of VRF on the UF processing of the juice is carried out according to the semi-batch configuration and for a TMP of 2 bars, a FF of 228 L/h and a temperature of 27°C. The figure 8 shows the variation of the permeation flux as a function of the VRF for the two membranes.

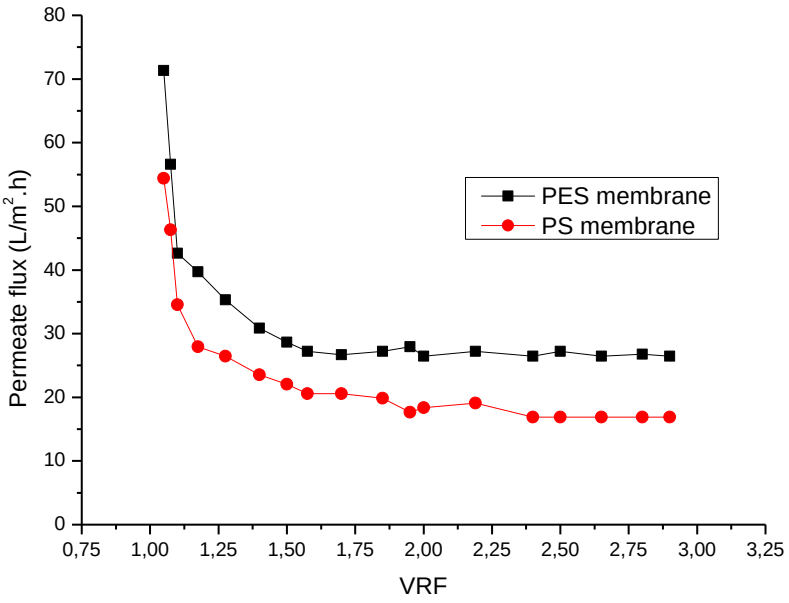

Figure 8: Variation of the permeation flux as a function of the VRF for the two membranes.

The permeate flux (Jp) of both membranes gradually decreases over VRF during this cross-flow filtration. This decline is attributed to concentration polarization and gel formation. Firstly, the permeate flux decreases rapidly due to concentration polarization. Then a slight decrease is observed until a VRF equal to 2, and finally the flux becomes stationary due to complete formation cake fouling on the membrane surface. During UF, polysaccharides, polyphenols and other colloidal substances accumulate on the membrane surface, forming a gel layer which in turn acts as a secondary membrane. This phenomenon causes a sharp decrease of the permeate flux at the start of the operation, then the permeate flux reaches a plateau. These observations corroborate with the results obtained by Cassano et al.(2004) and Constela et al.(1997) for the clarification of kiwi fruit juices, blood orange and apple juice.

B.2 Fouling Identification: Hermia Model

In order to determine the fouling mode responsible for permeate flux decline the study is-performed on the two membranes in semi-batch mode configuration. Then we consider the expressions of the flux relating to the four fouling mechanisms of Hermia model modified by Field et al. (2012), who inserted a deposit erosion parameter in the case of cross-flow filtration (Charfi et al.,2012). More precisely, the permeate flow is considered as a function of time, the value of the initial flow J_0 is set and the parameters K_{cf}, K_{pc}, K_{ib} and K_{cb} which correspond to each fouling mechanisms (cake formation, pore constriction, intermediate blockage, complete blockage) are optimized. These parameters have been optimized using the least squares method and their expressions obtained by analytical resolution of the model are respectively presented in equation (8):

$$K_{cf} = \frac{\alpha C \mu p}{\rho_s \Delta P}, \quad K_{ib} = \frac{C}{\rho_s h}, \quad K_{pc} = \frac{2CJ_0^{1/2}}{\rho_s e}, \quad K_{cb} = \frac{J_0}{\rho_s h} \qquad \text{(eq. 8)}$$

All those parameters are described in A. (Charfia et al., 2012).

Figure 9 shows the curves of the experimental and modeling data using Hermia model for both membranes. The parameters K_{cf}, K_{pc}, K_{ib} and K_{cb} obtained from the modeling of the fouling according to Hermia model are presented in the Table 5.

Table 5: Fouling modeling constants for the two membranes.

		n=0	n=3/2	n=1	n=2
PES	K_i	K_{cf} = 7.81 10^7	K_{pc} = 3.13	K_{ib} = 945.80	K_{cb} = 0.01
	R-square	0.82	0.38	0.60	0.07
PS	K_i	K_{cf} = 1.21 10^8	K_{pc} = 3.62	K_{ib} = 1198.68	K_{cb} = 0.01
	R-square	0.96	0.74	0.87	0.55

The R-squares obtained for the fitting of the 4 sealing modes for the PS membrane are better than those obtained by the PES membrane. The fitting of the cake formation fouling and intermediate blocking modes have the largest R-squares for the two membranes. Analysis of the values of the optimized parameter K_{cf} (cake

formation) and K_{ib} (intermediate blocking) reveals values similar to those reported in A. (Charfi et al.,2012) for UF membranes, the site of these fouling modes. The other optimized parameters K_{pc} and K_{cb} which indicate respectively the fouling modes of pore constriction and total blockage are markedly lower than those reported in the literature for UF membranes (Charfi et al.,2012). Indeed, the contribution of these types of fouling is negligible in our case. These results could be explained by the small size of the pores of these membranes and also by the nature of the organic substances presents in the juice solution to be treated, which promote surface fouling. These observations are in accordance with the results obtained by He et al., (2005) in short-term operation using four UF membranes coupled to an anaerobic bioreactor.

It appears that the fouling mechanism, which describes the experimental data for membranes tested is cake formation type. This fouling mode could be explained by the accumulation of retained molecules on the membrane surface due to the concentration polarization which gradually blocks the pores on the surface until equilibrium, at the same time the build-up of retained matter on the membrane surface lead to a cake formation. This build-up causes an increase in the hydraulic resistance of the system leading to permeate flux decline.

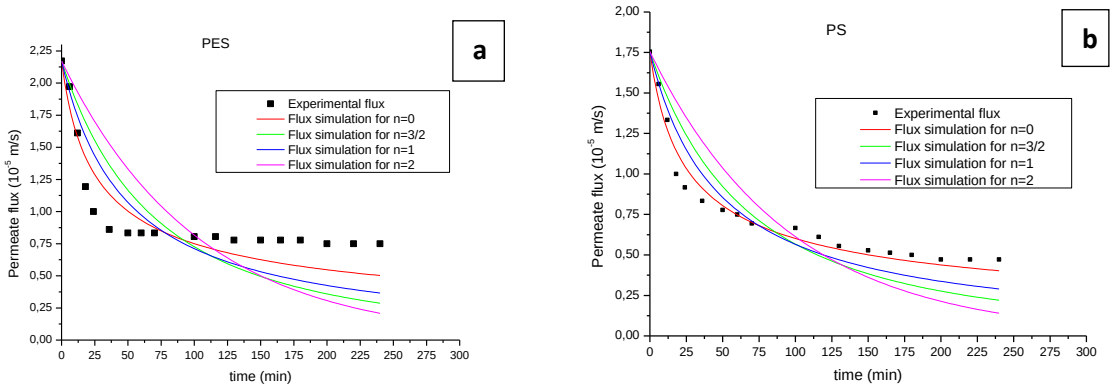

Figure 9: Experimental and modeling data using the Hermia model for PS (a) and PES (b) membranes.

B.3 Fouling Identification: Resistance Model

To quantify the resistance of the various fouling (internal and external) and to determine the resistance responsible of flux decline, the experimental method adopted consists in determining the total resistance of the membrane (R_t) after UF separation from the value of permeation flux measured based on Darcy's law. The total resistance R_t is the sum of the resistance of concentration polarization layer (R_c), the membrane resistance (R_m) and the fouling resistance (R_f) which is the sum of the reversible resistance R_{rev} and the irreversible resistance R_{irrev} of the membrane are presented in equation (9):

$$R_t = R_c + R_m + R_f \quad \text{with} \quad R_f = R_{rev} + R_{irrev} \qquad \text{(eq. 9)}$$

They are defined by the equation (10):

$$R_m = \frac{1}{\mu_w . L_P^0}, \quad R_t = \frac{1}{\mu_w . L_P^1}, \quad R_m + R_f = \frac{1}{\mu_w . L_P^2}, \quad R_m + R_{irrev} = \frac{1}{\mu_w . L_P^3} \qquad (eq. 10)$$

With:

μ_w the viscosity of pure water (Pa.s).

L_p^i: the permeability to pure water of the membrane ((L.m^{-2}.h^{-1}.bar^{-1}).

L_P^0 the permeability to pure water of the membrane before processing the juice.

L_P^1 the permeability to pure water of the membrane after processing the juice.

L_P^2 the permeability to pure water of the membrane after rinsing the membrane with water.

L_P^3 the permeability to pure water of the membrane after chemical cleaning of the membrane.

Table 6 shows the value of different types of resistance during juice UF. It appears that the total resistance for the PS membrane is higher than that for the PES membrane. The resistance of the concentration polarization layer is responsible of 63.8% for the PS membrane resistance and 52.2% for the PES total resistance. The fouling resistance contributes with 31.3% and 24.6% in the total resistance for PES and PS membrane respectively. These results confirm that the concentration polarization is the main cause of the flux drop.

Table 6: Calculated values of different resistances during UF of juice.

Resistance (m^{-1})	PES	PS
R_m	1.64 10^{12}	1.68 10^{12}
R_t	9.91 10^{12}	14.55 10^{12}
R_c	5.17 10^{12}	9.29 10^{12}
R_{rev}	3.02 10^{12}	3.5 10^{12}
R_{irrev}	0.08 10^{12}	0.08 10^{12}
R_m/R_t (%)	16.5%	11.5%
R_c/R_t (%)	52.2%	63.8%
R_f/R_t (%)	31.3%	24.6%

C. Effect of UF on chemical parameters of Valencia orange juice

The quality study of the effluent obtained after the treatment of the juice by UF is carried out according to the semi-batch configuration and for a TMP of 2 bars, a FF of 228 L/h, a VRF of 3 and a temperature of 27°C. Table 7

gives the physicochemical characteristics of the permeate. SS and AIS are completely removed from the juice which improves color and clarity. The TSS content of the permeate decreases slightly. Viscosity and density of the ultrafiltered juice are significantly reduced due to the removal of all SS and pectic matter. pH values vary slightly after UF treatment. The clarified juice obtained by UF for the two membranes has physicochemical and nutritional properties very similar to those of the Valencia orange juice feed, except for the absence of SS.

Table 7: Physicochemical characteristics of the permeate.

	Valencia orange juice depectinized	Permeate of PES membrane	Permeate of PS membrane
PH	3.32	3.30	3.29
Density (g/cm^3)	1.08	1.03	1.02
Viscosity (mPa.s)	1.45	1.04	1.03
Color (A_{420})	0.76	0.12	0.103
Clarity (%T_{660})	45.57	97.19	97.13
Acidity (%CA)	1.02	1.01	0.99
TSS (°Brix)	11.09	10.86	10.84
SS (W/W%)	4.12	6.01	6.01
AIS (Wt%)	0.19	0	0

As conclusion, the clarification of Moroccan Valencia orange juice has been studied by UF using flat sheet membranes with MWCO of 30 and 20 kDa respectively in cross-flow filtration mode. For both membranes, UF process is optimized by RSM based on a custom design. Permeate fluxes of 58.81 and 44.10 L/m^2.h were obtained respectively with the PES and PS membranes under optimal conditions, and with a desirability of almost 1. In addition, ANOVA shows a reliability of the data with a good correlation coefficient R^2 exceeding 0.96. In continuous mode, PES membrane exhibits a higher permeate flux than PS membrane. The behavior of PES membrane in reducing the compounds contributing to the quality of the juice is similar to that of PS membranes. According to the results, the two membranes make it possible to retain the original composition of the Moroccan Valencia orange juice in terms of the content of antioxidant compounds. The clarified juice obtained by UF for the two membranes has physicochemical and nutritional properties very similar to those of the Valencia orange juice feed, excepted for the absence of SS. Based on the permeate flow data and the chemical composition of the clarified juice, the most suitable membrane for the clarification of the juice is found to be the PES membrane. In semi-batch mode, the permeate flux decreases with the increase FRV for both membranes. The use of Hermia model allows identifying the fouling mechanism that occurs during UF processes. Calculation parameters of Hermia model shows that the mechanism, which describes experimental data for the two membranes, is a combination of two modes of

fouling: intermediate blocking and cake formation. On the other hand, the use of the resistance model has shown that the concentration polarization is the main cause of the flux drop.

REFERENCES

Addar. F.Z, El-Ghzizel.S, Tahaikt. M, Belfaquir. M, Taky. M, Elmidaoui.A.2021.Fluoride removal by nanofiltration: experimentation, modelling and prediction based on the surface response method. J. Desalination and Water Treatment, 240 :75–88.

Arriola. N.A., Santos. G.D, Prudêncio. E.S, Vitali. L, Petrus .J.C.C, Castanho Amboni R.D.M 2014. Potential of nanofiltration for the concentration of bioactive compounds from watermelon juice, Int. J. Food Sci. Technol. 49: 2052–2060. doi:10.1111/ijfs.12513.

Bining. J, Alfredo. C, E. Drioli 2004. Recent advances on membrane processes for the concentration of fruit juices: A review. J. Food Eng. 63: 303–324. doi:10.1016/j.jfoodeng.2003.08.003.

Boumaaza. M, Belaadi. A & Bourchak.M.2020.The Effect of Alkaline Treatment on Mechanical Performance of Natural Fibers-reinforced Plaster: Optimization Using RSM, Journal of Natural Fibers. doi: 10.1080/15440478.2020.1724236

Box. G. E. P, Draper .R. N. (2007). Response surfaces, Mixtures and Ridge Analyses, Second Edition, Wiley and Sons,New York.

Carmela. C, Enrico. D, Alfredo. C 2020. Perspective of membrane technology in pomegranate juice processing: A review, Foods. 9: 1–25. doi:10.3390/foods9070889.

Carneiro. L, Dos Santos Sa.I, Dos Santos Gomes.F, Matta .V.M, Cabral. L.M.C. Cold 2002 sterilization and clarification of pineapple juice by tangential microfiltration, Desalination. 148: 93–98. doi:10.1016/S0011-9164(02)00659-8.

Cassano .A, Conidi .C, Drioli. E 2011. Clarification and concentration of pomegranate juice (Punica granatum L.) using membrane processes, J. Food Eng. 107: 366–373. doi:10.1016/j.jfoodeng.2011.07.002.

Cassano.A, Drioli.E, Galaverna.G, Marchelli.R, Di Silvestro.G, Cagnasso. P 2003. Clarification and concentration of citrus and carrot juices by integrated membrane processes, J. Food Eng. 57: 153–163. doi:10.1016/S0260-8774(02)00293-5.

Cassano .A, Conidi .C, Timpone .R, D'Avella .M, Drioli. E 2007. A membrane-based process for the clarification and the concentration of the cactus pear juice. J. Food Eng. 80: 914–921. doi:10.1016/j.jfoodeng.2006.08.005.

Cassano.A, Figoli. A, Tagarelli. A, Sindona.G, Drioli.E.2006, Integrated membrane process for the production of highly nutritional kiwifruit juice. Desalination. 189:21–30. doi:10.1016/j.desal.2005.06.009.

Cassano.A, Jiao.B , Drioli.E.2004.Production of concentrated kiwifruit juice by integrated membrane process, Food Res. Int. 37 :139–148. doi:10.1016/j.foodres.2003.08.009.

Cassano.A, Marchio.M, Drioli.E.2007.Clarification of blood orange juice by ultrafiltration: analyses of operating parameters, membrane fouling and juice quality, Desalination. 212:15–27. doi:10.1016/j.desal.2006.08.013.

Charfi. A, Ben Amar.N, Harmand.J.2012.Analysis of fouling mechanisms in anaerobic membrane bioreactors, Water Res. 46 :2637–2650. doi:10.1016/j.watres.2012.02.021.

Chen .X, Zhao. X, Gao .Y, Yin J, Bai. M, Wang.F.2018.Green synthesis of gold nanoparticles using carrageenan oligosaccharide and their in vitro antitumor activity. Mar. Drugs, 277 :16(8). https:// doi.org/10.3390/md16080277.

Constenla. D.T, Lozano .J.E.H ollow fibre ultrafiltration of apple juice: Macroscopic approach, LWT - Food Sci. Technol. 30:373–378.doi:10.1006/fstl.1996.0192.

Dave. M, Khoiruddinb.K, I.G. Wenten 2018. Beverage dealcoholization processes: Past, present, and future, Trends Food Sci. Technol. 71: 36–45. doi:10.1016/j.tifs.2017.10.018.

Dessie Y, Tadesse.S, Eswaramoorthy.R.2020.Physicochemical parameter influences and their optimization on the biosynthesis of MnO2 nanoparticles using Vernonia amygdalina leaf extract. Arab J Chem,13:6472–6492.https://doi.org/10.1016/j.arabjc.2020.06.006

Enrico D, Lidietta. G, Enrica. F.2017. Comprehensive Membrane Science and Engineering, in: Enrico Drioli, L. Giorno, E. Fontananova (Eds.). Ultrafiltr. Fundam. Eng., 2nd ed., Elsevier Science.

Gulec. H.A, Bagci.P.O, Bagci.U.2018.Performance enhancement of ultrafiltration in apple juice clarification via low-pressure oxygen plasma: A comparative evaluation versus pre-flocculation treatment, LWT - Food Sci. Technol. 91: 511–517. doi:10.1016/j.lwt.2018.01.082.

He.Y, Xu.P, Li.C, Zhang.B.2005.High-concentration food wastewater treatment by an anaerobic membrane bioreactor, Water Res. 39: 4110–4118. doi:10.1016/j.watres.2005.07.030.

Hussain S, Khan.H, Gul S.S, Steter J.R, Motheo.A.J.2021.Modeling of photolytic degradation of sulfamethoxazole using boosted regression tree (BRT), artificial neural network (ANN) and response surface methodology (RSM); energy consumption and intermediates study Chemosphere. 276. Article 130151.

Khuri.A. I., Cornell J. A. (1996). Response surfaces. Designs and analyses (2nd edition), Statistics: Textbooks and Monographs 152, New York, NY: Marcel Dekker

Lin W, Jing.L, Zhang.B.2020.Micellar-Enhanced Ultrafiltration to Remove Nickel Ions: A Response Surface Method and Artificial Neural Network Optimization Water., 12: 1269.

Liu J, Wang J, Leung.C, Gao.F.2018. A multi-parameter optimization model for the evaluation of shale gas recovery enhancement, Energies, 654:11(3).

Maghsoudy N, Azar P.A, Tehrani. M.S, Husain .S.W, Larijani.K.2019.Biosynthesis of Ag and Fe nanoparticles using Erodium cicutarium; study, optimization, and modeling of the antibacterial properties using response surface methodology. J. Nanostruct. Chem. 9:203–216.https://doi.org/10.1007/s40097-019-0311-z.

Medina. B.G, Garcia A. 1988, Concentration of orange juice by reverse osmosis. J. Food Process Eng. 10: 217–230. doi:10.1111/j.1745-4530.1988.tb00014.x.

Mondal P, Purkait.M.K. 2017. Green synthesized iron nanoparticleembedded pH-responsive PVDF-co-HFP membranes: Optimization study for NPs preparation and nitrobenzene reduction. Sep.Sci. Technol. 52: 2338–2355. https://doi.org/10.1080/ 01496395.2016.1274759.

Montgomery. D.C, 2001. Design and Analysis of Experiments, 5th ed., John Wiley &Sons, New York.

Myers. R.H, Montgomery. D.C.2002.Response Surface Methodology: Process and Product Optimization Using Designed Experiments, 2nd ed., John Wiley & Sons, New York. https://doi.org/10.3390/ en11030654.

Najafi.B, Faizollahzadeh Ardabili S, Shamshirband S, Chau & T Rabczuk.K .2018.Application of ANNs, ANFIS and RSM to estimating and optimizing the parameters that affect the yield and cost of biodiesel production.Engineering Applications of Computational Fluid Mechanics.121:611-624.Doi: 10.1080/19942060.2018.1502688.

Nilsson.J.L.1990., Protein fouling of uf membranes: Causes and consequences. J. Memb. Sci. 52:121–142.doi:10.1016/S0376-7388(00)80481-0.

Noble R.D, Stern. S. 1st Edition, 1995., Membrane Separations Technology.https://www.elsevier.com/books/membrane-separations-technology/noble/978-0-444-81633-7 (accessed October 10, 2020).

Omar J.M, Nor. M.Z.M., Basri M.S.M, Che Pa. N.F.2020. Clarification of guava juice by an ultrafiltration process: Analysis on the operating pressure, membrane fouling and juice qualities, Food Res. 4 :85–92.doi:10.26656/fr.2017.4 (S1).S30.

Qaid.S, Zait.M, EL Kacemi.K, EL Midaoui.A, EL Hajji.H, Taky.M. 2017.Ultrafiltration for clarification of Valencia orange juice: Comparison of two flat sheet membranes on quality of juice production.J. Mater. Environ. Sci. 8 :1186–1194.

Toledo Guimarães. J, Silva E.K, Freitas. M.Q, Almeida Meireles. M.A, Cruz. A.G 2018. Non-thermal emerging technologies and their effects on the functional properties of dairy products. Curr. Opin. Food Sci. 22: 62–66. doi:10.1016/j.cofs.2018.01.015.

Received: 16th December 2021; Accepted: 06th Juny 2022; First distribution: 18th October 2022